



Published in final edited form as:

Nature. 2013 July 4; 499(7456): 43–49. doi:10.1038/nature12222.

COMPREHENSIVE MOLECULAR CHARACTERIZATION OF CLEAR CELL RENAL CELL CARCINOMA

The Cancer Genome Atlas Research Network

Abstract

Genetic changes underlying clear cell renal cell carcinoma (ccRCC) include alterations in genes controlling cellular oxygen sensing (e.g. *VHL*) and the maintenance of chromatin states (e.g. *PBRM1*). We surveyed more than 400 tumors using different genomic platforms and identified 19 significantly mutated genes. The PI3K/Akt pathway was recurrently mutated, suggesting this pathway as a potential therapeutic target. Widespread DNA hypomethylation was associated with mutation of the H3K36 methyltransferase *SETD2*, and integrative analysis suggested that mutations involving the SWI/SNF chromatin remodeling complex (*PBRM1*, *ARID1A*, *SMARCA4*) could have far-reaching effects on other pathways. Aggressive cancers demonstrated evidence of a metabolic shift, involving down-regulation of genes involved in the TCA cycle, decreased AMPK and PTEN protein levels, up-regulation of the pentose phosphate pathway and the glutamine transporter genes, increased acetyl-CoA carboxylase protein, and altered promoter methylation of *miR-21* and *GRB10*. Remodeling cellular metabolism thus constitutes a recurrent pattern in ccRCC that correlates with tumor stage and severity and offers new views on the opportunities for disease treatment.

Kidney cancers, or renal cell carcinomas (RCC), are a common group of chemotherapy resistant diseases that can be distinguished by histopathological features and underlying gene mutations.¹ Inherited predisposition to RCC has been shown to arise from genes involved in regulating cellular metabolism, making RCC a model for the role of an oncologic-metabolic shift, commonly referred to as the “Warburg effect”, leading to malignancy.² The most common type of RCC, clear cell renal cell carcinoma (ccRCC), is closely associated with *VHL* gene mutations that lead to stabilization of hypoxia inducible factors (*HIF-1 α* and *HIF-2 α*) in both sporadic and familial forms. *PBRM1*, a subunit of the PBAF SWI/SNF chromatin remodeling complex, as well as histone deubiquitinase *BAP1* and histone methyltransferase *SETD2*, were recently found to be altered in 41%, 15% and 12% of ccRCCs, respectively^{3–5}, implicating major roles for epigenetic regulation of additional functional pathways participating in the development and progression of the disease. Oncogenic metabolism and epigenetic reprogramming have thus emerged as central features of ccRCC.

Users may view, print, copy, download and text and data- mine the content in such documents, for the purposes of academic research, subject always to the full Conditions of use: http://www.nature.com/authors/editorial_policies/license.html#terms

²⁶The Center for Biomedical Informatics, Harvard Medical School, Boston, MA 02115 USA.

DATA ACCESS STATEMENT:

All of the primary sequence files are deposited in CGHub (File IDs in Data File S1) and all other data are deposited at the Data Coordinating Centrer (DCC) for public access (<http://cancergenome.nih.gov/>).

In the present study, clinical and pathological features, genomic alterations, DNA methylation profiles, and RNA and proteomic signatures were evaluated in ccRCC. We accrued more than 500 primary nephrectomy specimens from patients with histologically confirmed ccRCC that conformed to the requirements for genomic study defined by the Cancer Genome Atlas (TCGA)⁶, together with matching ‘normal’ genomic material. Samples were restricted to those that contained at least 60% tumor nuclei, (median 85%) by pathological review (clinical data summary provided in Table S1). A data freeze representing 446 samples was generated from at least one analytical platform (‘Extended’ data set) and data from all platforms were available for 372 samples for coordinated, integrative analyses (‘Core’ data set)(Data File S1, Table S2). No substantial batch effects in the data that might confound analyses were detected (Figures S1–S20).

Somatic Alterations

The global pattern of somatic alterations, determined from analysis of 417 samples, is shown in Figure 1A. DNA hybridizations showed that recurrent arm-level and focal somatic copy number alterations (SCNAs) occurred at a fewer sites than is generally observed in other cancers ($p < 0.0004$; Figures S21–S22, Table S3). However, SCNAs that were observed more commonly involved entire chromosomes or chromosome arms, rather than focal events (17% vs 0.4%, Figure 1b). Notably, the most frequent arm-level events involved loss of chromosome 3p³ (91% of samples), encompassing all of the four most commonly mutated genes (*VHL*, *PBRM1*, *BAP1* and *SETD2*).

The data also suggested lower and more variable tumor cellularity⁷ in the accrued samples, compared to conventional pathological review (median 54% ± 14%). This may reflect stromal or endothelial cell contributions, or tumor cell heterogeneity. A recent study of multiple samples from single tumors has demonstrated significant regional genomic heterogeneity, but with shared mutations in frequently mutated genes and convergent evolution of other common gene level events.⁸ The mutation frequencies of key genes (*VHL*, *PBRM1*, etc.), as well as copy number gains and losses found here, were, however, consistent with previous reports. Tumor purity was therefore not determined to be a limitation in the current study.

Arm level losses on chromosome 14q, associated with loss of *HIF1A*, which has been predicted to drive more aggressive disease⁹, were also frequent (45% of samples). Gains of 5q were observed (67% of samples) and additional focal amplifications refined the region of interest to 60 genes in 5q35, which was particularly informative as little has been known about the importance of this region in ccRCC since the 5q gain was initially described. Focal amplification also implicated the protein kinase C member, *PRKCF*⁵ and the MDS1 and EVI1 complex locus *MECOM* at 3p26, the p53 regulator *MDM4* at 1q32, *MYC* at 8q24 and *JAK2* on 9p24. Focally deleted regions included the tumor suppressor genes *CDKN2A* at 9p21 and *PTEN* at 10q23, putative tumor suppressor genes *NEGR1* at 1p31, *QKI* at 6q26, and *CADM2* at 3p12 and the genes that are frequently deleted in cancer, *PTPRD* at 9p23 and *NRXN3* at 14q24.¹⁰

Whole exome sequencing (WES) of tumors from 417 patients identified 36,353 putative somatic mutations, including 16,821 missense mutations, 6,383 silent mutations and 2,999 indels, with an average of 1.1 ± 0.5 non-silent mutations per megabase (Figures S23–S25). Mutations from 50 genes with high apparent somatic mutation frequencies (Table S4) were independently validated using alternative sequencing instrumentation (Figure S26). In tumors from 22 patients, whole genome sequencing was also used to validate and calibrate the WES data and confirmed 83% of the WES mutation-calls (Tables S5–S6). In line with results of previous studies (Tables S7–S8), the validated mutation data identified nineteen significantly mutated genes (SMGs) ($q < 0.1$), with *VHL*, *PBRM1*, *SETD2*, *KDM5C*, *PTEN*, *BAP1*, *MTOR* and *TP53* representing the eight most extreme members ($q < 0.00001$) (Figure 1a). Eleven additional SMGs were of considerably lower significance ($q < 0.1 - 0.5$) but included known cancer genes. Among all SMGs, only mutation of *BAP1* correlated with poor survival outcome (Figure S27). Approximately 20% of cases had none of the 19 recorded SMGs, although many contained rare mutations in other known oncogenes or tumor suppressors, involving survival associations, illustrating the genetic complexity of ccRCC⁸ (Figures S28–S30 and Table S9).

Eighty-four putative RNA fusions were identified in 416 ccRCC samples.¹¹ Eleven of thirteen predicted events (Figure 1c) were validated using targeted methods, consistent with an 85% true-positive rate (Table S10 and Figures S31–S35). A recurrent *SFPQ-TFE3* fusion (previously linked to non-clear cell translocation-associated RCC¹²) was found in five samples, all of which were *VHL* wildtype, indicating either that these tumors are a clear cell variant or that translocation-associated renal tumors may be histologically indistinguishable from conventional ccRCC. Furthermore, the TFE3 protein as well as an X(p11) rearrangement was found in three of those samples, where there were available slides.

DNA Methylation Profiles

We observed epigenetic silencing of *VHL* in about 7% of ccRCC tumors, which was mutually exclusive with mutation of *VHL* (Figure 1a), reflecting the central role of this locus in ccRCC.¹³ An additional 289 genes displayed evidence of epigenetic silencing in at least 5% of tumors. The top-ranked gene by inverse correlation between gene expression and DNA methylation was *UQCRH*, hypermethylated in 36% of the tumors. *UQCRH* has been previously suggested to be a tumor suppressor¹⁴, but not linked to ccRCC. Interestingly, increasing promoter hypermethylation frequency correlated with higher stage and grade (Figure 2a, b).

We also evaluated the global consequences of mutation in specific epigenetic modifiers. Mutations in *SETD2*, a non-redundant H3K36 methyltransferase, were associated with increased loss of DNA methylation at non-promoter regions (Figures 2c, 2d). This discovery is consistent with the emerging view that H3K36 trimethylation may be involved in the maintenance of a heterochromatic state¹⁵, whereby DNA methyltransferase 3A (DNMT3A) binds H3K36me3 and methylates nearby DNA.¹⁶ Thus, reductions of H3K36me3 through *SETD2* inactivation could lead indirectly to regional loss of DNA methylation.

RNA Expression

Unsupervised clustering methods identified four stable subsets in both mRNA (m1–m4) and miRNA (mi1–mi4) expression datasets (Figures 3a, S36–S39). Supervised clustering revealed the similarity of these new mRNA classes to the previously reported ccA and ccB expression subtypes¹⁷, with cluster m1 corresponding to ccA and ccB divided between m2 and m3 (Table S11). Cluster m4 probably accounts for the roughly 15% of tumors previously unclassified in the ccA/ccB classification scheme. Similarly, the survival advantage previously observed for ccA cases was again identified for m1 tumors (Figure 3b).

The m1-subtype was characterized by gene sets associated with chromatin remodeling processes and a higher frequency of *PBRM1* mutations (39% in m1 vs 27% in others, $p=0.027$). Deletion of *CDKN2A* (53% vs 26%; $p<0.0001$) and mutations in *PTEN* (11% vs 1%; $p<0.0001$) were more frequent in m3 tumors (Figure S5). The m4 group displayed higher frequencies of *BAP1* mutations (17% vs 7%; $p=0.002$) and base excision repair; however, this group also harbored more *mTOR* mutations (12% vs 4%; $p=0.01$) and ribosomal gene sets.

Survival differences evident in miRNA-based subtypes (Figures S40–S44) correlated with the mRNA data (Figures 3b–d). For example, miR-21, previously shown to demonstrate strong regulatory interactions in ccRCC¹⁸ and with established roles in metabolism^{15,19,20} correlated strongly with worse outcome, and DNA promoter methylation levels inversely correlated with expression of miR-21, miR-10b, and miR-30a (Table S12–S14). miRNA interactions thus represent a significant component of the epigenetic regulation observed in ccRCC.

Integrative data analyses

We used a combination of approaches for integrative pathway analysis. The HotNet²¹ algorithm employs a heat diffusion model, to find subnetworks distinguished by *both* the frequency of mutation in genes (nodes in the network) and the topology of interactions between genes (edges in the network). In ccRCC, Hotnet identified twenty-five subnetworks of genes within a genome-scale protein-protein interaction network (Table S15 and Figure S45). The largest and most frequently mutated network contained *VHL* and interacting partners. The second most frequently mutated subnetwork included *PBRM1*, *ARID1A* and *SMARCA4*, key genes in the PBAF *SWI/SNF* chromatin remodeling complex.

We also inferred activities for known pathways, by using the PARADIGM algorithm to incorporate mutation, copy, and mRNA expression data, with pathway information catalogued in public databases. This method identified a highly significant subnetwork of 2,398 known regulatory interactions, connecting 1,218 molecular features (645 distinct proteins) (Figures S46–S49, Tables S16–S17). Several “active” transcriptional “hubs” were identified, by searching for transcription factors with targets that were inferred to be active in the PARADIGM network. The active hubs found included HIF/ARNT, the transcription factor program activated by *VHL* mutation, as well as MYC/Max, SP1, FOXM1, JUN, and FOS. Together, these hubs and several less well-studied transcription factors, interlink much

of the transcriptional program promoting glycolytic shift, de-differentiation, and growth promotion in ccRCC.

We next searched for causal regulatory interactions connecting ccRCC somatic mutations to these transcriptional hubs, using a bi-directional extension to HotNet ('TieDIE') and identified a chromatin-specific sub-network (Figures 4a, S50–S52). TieDIE defines a set of transcriptional targets, whose state in the tumor cells is hypothesized to be influenced by one or more of the significantly mutated genes. The chromatin modification pathway intersects a wide variety of processes, including the regulation of hormone receptors (e.g. *ESR1*), RAS signaling via the *SRC* homolog (*SHC1*), immune-related signaling (e.g. *NFκB1* and *IL6*)²⁶, transcriptional output (e.g. *HIF1A*, *JUN*, *FOS*, and *SP1*), *BRCA1* function (via *BAP1*) and Beta-catenin (*CTNNB1*) and TGF-beta (*TGFBR2*) signaling via interactions with a *SMARC-PBRM1-ARID1A* complex. The complexity of these interactions reflects the potential for highly pleiotropic effects following primary events in chromatin modification genes.

The mutations in the chromatin regulators *PBRM1*, *BAP1*, and *SETD2* were differentially associated with altered expression patterns of large numbers of genes when compared to samples bearing a background of *VHL* mutation (Table S18–S21, Figure S53). Each chromatin regulator had a distinct set of downstream effects, reflecting diverse roles for chromatin remodeling in the transcriptome.

Additionally, an unsupervised pathway analysis using the MEMo algorithm²², identified mutually exclusive patterns of alterations targeting multiple components of the PI3K/Akt/mTOR pathway in 28% of the tumors (Figures 4b, Table S22). Interestingly, the altered gene module included two genes from the broad amplicon on 5q35.3: *GNB2L1/RACK1* and *SQSTM1/p62*. Both these genes have previously been associated with activation of PI3K signaling^{23,24}. Furthermore, mRNA expression levels of these two genes were correlated with both DNA copy number level increases and alteration status of the PI3K pathway (Figures S54–S55). The mutual exclusivity module also includes frequent over-expression of EGFR, which correlates with increased phosphorylation of the receptor (Figure S56), and which has been previously associated with Lapatinib response in ccRCC²⁵.

Correlations with survival

Where unsupervised analyses had indicated that common molecular patterns were associated with patient survival, we sought to further define molecular prognostic signatures at the levels of mRNA, miRNA, DNA methylation, and protein. Data were divided into 'discovery' (N=193) and 'validation' (N=253) sets and platform-specific signatures were defined using Cox analyses²⁶. Kaplan-Meier analysis for each signature showed statistically significant associations with survival in the validation subset (Figures 5a and S57). Multivariate Cox analyses, incorporating established clinical variables, showed that the mRNA, miRNA, and protein signatures provided additional prognostic power (Table S23). In addition, these signatures could provide molecular clues as to the drivers of aggressive cancers.

Top protein correlates of worse survival included reduced AMP-activated kinase (AMPK) and increased acetyl-CoA carboxylase (ACC) (Figure S58). Together, down-regulation of

AMPK and up-regulation of ACC activity contribute to a metabolic shift towards increased fatty acid synthesis.²⁷ A metabolic shift to an altered use of key metabolites and pathways was also apparent when considering the full set of genes involved in the core metabolic processes, including a shift towards a “Warburg effect”-like state (Figure 5b). Poor prognosis correlated with down-regulation of AMPK complex and the Krebs cycle genes, and with up-regulation of genes involved in the pentose phosphate pathway (*G6PD*, *PGLS*, *TALDO*, *TKT*) and fatty acid synthesis (*FASN*, *ACC*).

Examination of potential genetic or epigenetic drivers of a glycolytic shift led us to identify methylation events involving *miR-21* and *GRB10*, with decreased promoter methylation of each gene (thereby higher expression) being associated with worse or better outcome, respectively (Figure 5B, Figure S59, Table S24). Both genes regulate the PI3K pathway: *miR-21* is inducible by high glucose levels and down-regulates PTEN²⁰; while the tumor suppressor Grb10 negatively regulates PI3K and insulin signaling.²⁸ Promoter methylation of *miR-21* and *GRB10* were coordinated with their mRNA expression patterns, as well as with the mRNA expression of other key genes and protein expression in the metabolic pathways (Figures 5C and S60). In addition to the PI3K pathway (Figures 5B and S61), molecular survival correlations involved several pro-metastatic matrix metalloproteinases (Figure S62).

Discussion

Our study sampled a single site of the primary tumor, in a disease with a potentially high level of tumor heterogeneity⁸. The extent to which convergent evolutionary events are a common theme in ccRCC remains to be determined, but may indicate that critical genes will be represented across the tumor landscape for an individual mass. In general, the large sample size appeared to overcome the intrinsic challenges of studying a genetically complex disease, revealing rare variants at rates similar to what has been described previously²⁹. The samples, taken from primary tumor specimens, were reflective of patients fit for either definitive or cytoreductive nephrectomy, while future work could explore the genomic landscape of metastatic lesions.

Pathway and integrated analyses highlighted the importance of the well-known *VHL/HIF* pathway, the newly emerging chromatin remodeling/histone methylation pathway, and the *PI3K/AKT* pathway. The observation of chromatin modifier genes being frequently mutated in ccRCC strongly supports the model of nucleosome dynamics providing a key function in renal tumorigenesis. Although the mechanistic details remain to be defined as to how such modulation promotes tumor formation, the data presented here revealed alterations in DNA methylation associated with *SETD2* mutations. As an epigenetic process that can potentially alter many transcriptional outputs, these mutational events have the potential to alter the landscape of the tumor genome via altered expression of global sets of genes and genetic elements. Molecular correlates of patient survival further implicated PI3K/AKT as having a role in tumor progression, involving specific DNA methylation events. The PI3K/AKT pathway presents a strong therapeutic target in ccRCC, supporting the potential value of MTOR and/or related pathway inhibitor drugs for this cancer.^{30,31}

Cross-platform molecular analyses indicated a correlation between worsened prognosis in patients with ccRCC and a metabolic shift involving increased dependence on the pentose phosphate shunt, decreased AMPK, decreased Krebs cycle activity, increased glutamine transport and fatty acid production. These findings are consistent with the isotopomer spectral analysis of a pair of *VHL* $-/-$ clear cell kidney cancer cell lines, both of which were notably derived from patients with aggressive, metastatic disease, which revealed a dependence on reductive glutamine metabolism for lipid biosynthesis.³² The metabolic shift identified in poor prognosis ccRCC remarkably mirrors the Warburg metabolic phenotype (increased glycolysis, decreased AMPK, glutamine dependent lipogenesis) identified in type 2 papillary kidney cancer characterized by mutation of the Krebs cycle enzyme, fumarate hydratase.³² Further studies to dissect out the role of the commonly mutated chromosome 3 chromatin remodeling genes, PBRM1, SETD2 and BAP1, in ccRCC tumorigenesis and their potential role in the metabolic remodeling associated with progression of this disease will hopefully provide the foundation for the development of effective forms of therapy for this disease.

Methods Summary

Specimens were obtained from patients, with appropriate consent from institutional review boards. Using a co-isolation protocol, DNA and RNA were purified. In total, 446 patients were assayed on at least one molecular profiling platform, which platforms included: (1) RNA sequencing; (2) DNA methylation arrays; (3) miRNA sequencing; (4) Affymetrix SNP arrays; (5) exome sequencing; and (6) reverse phase protein arrays. As described above and in the Supplemental Methods, both single platform analyses and integrated cross-platform analyses were performed.

Supplementary Material

Refer to Web version on PubMed Central for supplementary material.

Acknowledgments

We wish to thank all patients and families who contributed to this study. A full list of grant support and acknowledgments is included in the supplement.

Reference List

1. Linehan WM, Walther MM, Zbar B. The genetic basis of cancer of the kidney. *The Journal of urology*. 2003; 170:2163–2172.10.1097/01.ju.0000096060.92397.ed [PubMed: 14634372]
2. Linehan WM, Srinivasan R, Schmidt LS. The genetic basis of kidney cancer: a metabolic disease. *Nature reviews. Urology*. 2010; 7:277–285.10.1038/nrurol.2010.47 [PubMed: 20448661]
3. Zbar B, Brauch H, Talmadge C, Linehan M. Loss of alleles of loci on the short arm of chromosome 3 in renal cell carcinoma. *Nature*. 1987; 327:721–724.10.1038/327721a0 [PubMed: 2885753]
4. Guo G, et al. Frequent mutations of genes encoding ubiquitin-mediated proteolysis pathway components in clear cell renal cell carcinoma. *Nature genetics*. 2012; 44:17–19.10.1038/ng.1014 [PubMed: 22138691]
5. Eder AM, et al. Atypical PKC α contributes to poor prognosis through loss of apical-basal polarity and cyclin E overexpression in ovarian cancer. *Proceedings of the National Academy of Sciences of*

- the United States of America. 2005; 102:12519–12524.10.1073/pnas.0505641102 [PubMed: 16116079]
6. Wienholds E, Koudijs M, van Eeden F, Cuppen E, Plasterk R. The microRNA-producing enzyme Dicer1 is essential for zebrafish development. *Nature genetics*. 2003; 35:217–218. [PubMed: 14528306]
 7. Carter SL, et al. Absolute quantification of somatic DNA alterations in human cancer. *Nature biotechnology*. 2012; 30:413–421.10.1038/nbt.2203
 8. Gerlinger M, et al. Intratumor heterogeneity and branched evolution revealed by multiregion sequencing. *The New England journal of medicine*. 2012; 366:883–892.10.1056/NEJMoa1113205 [PubMed: 22397650]
 9. Shen C, et al. Genetic and functional studies implicate HIF1alpha as a 14q kidney cancer suppressor gene. *Cancer discovery*. 2011; 1:222–235.10.1158/2159-8290.CD-11-0098 [PubMed: 22037472]
 10. Herbers J, et al. Significance of chromosome arm 14q loss in nonpapillary renal cell carcinomas. *Genes, chromosomes & cancer*. 1997; 19:29–35. [PubMed: 9135992]
 11. Lewis B, Shih I, Jones-Rhoades M, Bartel D, Burge C. Prediction of mammalian microRNA targets. *Cell*. 2003; 115:787–798. [PubMed: 14697198]
 12. Clark J, et al. Fusion of splicing factor genes PSF and NonO (p54nrb) to the TFE3 gene in papillary renal cell carcinoma. *Oncogene*. 1997; 15:2233–2239.10.1038/sj.onc.1201394 [PubMed: 9393982]
 13. Herman JG, et al. Silencing of the VHL tumor-suppressor gene by DNA methylation in renal carcinoma. *Proceedings of the National Academy of Sciences of the United States of America*. 1994; 91:9700–9704. [PubMed: 7937876]
 14. Modena P, et al. UQCRH gene encoding mitochondrial Hinge protein is interrupted by a translocation in a soft-tissue sarcoma and epigenetically inactivated in some cancer cell lines. *Oncogene*. 2003; 22:4586–4593.10.1038/sj.onc.1206472 [PubMed: 12881716]
 15. Wagner EJ, Carpenter PB. Understanding the language of Lys36 methylation at histone H3. *Nature reviews. Molecular cell biology*. 2012; 13:115–126.10.1038/nrm3274 [PubMed: 22266761]
 16. Dhayalan A, et al. The Dnmt3a PWWP domain reads histone 3 lysine 36 trimethylation and guides DNA methylation. *The Journal of biological chemistry*. 2010; 285:26114–26120.10.1074/jbc.M109.089433 [PubMed: 20547484]
 17. Brannon AR, et al. Molecular Stratification of Clear Cell Renal Cell Carcinoma by Consensus Clustering Reveals Distinct Subtypes and Survival Patterns. *Genes & cancer*. 2010; 1:152–163.10.1177/1947601909359929 [PubMed: 20871783]
 18. Liu H, et al. Identifying mRNA targets of microRNA dysregulated in cancer: with application to clear cell Renal Cell Carcinoma. *BMC systems biology*. 2010; 4:51.10.1186/1752-0509-4-51 [PubMed: 20420713]
 19. Creighton CJ, et al. Integrated analyses of microRNAs demonstrate their widespread influence on gene expression in high-grade serous ovarian carcinoma. *PloS one*. 2012; 7:e34546.10.1371/journal.pone.0034546 [PubMed: 22479643]
 20. Dey N, et al. MicroRNA-21 orchestrates high glucose-induced signals to TOR complex 1, resulting in renal cell pathology in diabetes. *The Journal of biological chemistry*. 2011; 286:25586–25603.10.1074/jbc.M110.208066 [PubMed: 21613227]
 21. Vandin F, Upfal E, Raphael BJ. Algorithms for detecting significantly mutated pathways in cancer. *Journal of computational biology: a journal of computational molecular cell biology*. 2011; 18:507–522.10.1089/cmb.2010.0265 [PubMed: 21385051]
 22. Ciriello G, Cerami E, Sander C, Schultz N. Mutual exclusivity analysis identifies oncogenic network modules. *Genome research*. 2012; 22:398–406.10.1101/gr.125567.111 [PubMed: 21908773]
 23. He X, Wang J, Messing EM, Wu G. Regulation of receptor for activated C kinase 1 protein by the von Hippel-Lindau tumor suppressor in IGF-I-induced renal carcinoma cell invasiveness. *Oncogene*. 2011; 30:535–547.10.1038/onc.2010.427 [PubMed: 20871634]
 24. Duran A, et al. p62 is a key regulator of nutrient sensing in the mTORC1 pathway. *Molecular cell*. 2011; 44:134–146.10.1016/j.molcel.2011.06.038 [PubMed: 21981924]

25. Ravaud A, et al. Lapatinib versus hormone therapy in patients with advanced renal cell carcinoma: a randomized phase III clinical trial. *J Clin Oncol*. 2008; 26:2285–2291. [PubMed: 18467719]
26. Cancer Genome Atlas Research N. Integrated genomic analyses of ovarian carcinoma. *Nature*. 2011; 474:609–615.10.1038/nature10166 [PubMed: 21720365]
27. Tong WH, et al. The glycolytic shift in fumarate-hydratase-deficient kidney cancer lowers AMPK levels, increases anabolic propensities and lowers cellular iron levels. *Cancer cell*. 2011; 20:315–327.10.1016/j.ccr.2011.07.018 [PubMed: 21907923]
28. Yu Y, et al. Phosphoproteomic analysis identifies Grb10 as an mTORC1 substrate that negatively regulates insulin signaling. *Science*. 2011; 332:1322–1326.10.1126/science.1199484 [PubMed: 21659605]
29. Dalgliesh GL, et al. Systematic sequencing of renal carcinoma reveals inactivation of histone modifying genes. *Nature*. 2010; 463:360–363.10.1038/nature08672 [PubMed: 20054297]
30. Motzer RJ, et al. Efficacy of everolimus in advanced renal cell carcinoma: a double-blind, randomised, placebo-controlled phase III trial. *Lancet*. 2008; 372:449–456.10.1016/S0140-6736(08)61039-9 [PubMed: 18653228]
31. Hudes G, et al. Temsirolimus, interferon alfa, or both for advanced renal-cell carcinoma. *The New England journal of medicine*. 2007; 356:2271–2281.10.1056/NEJMoa066838 [PubMed: 17538086]
32. Metallo CM, et al. Reductive glutamine metabolism by IDH1 mediates lipogenesis under hypoxia. *Nature*. 2012; 481:380–384.10.1038/nature10602 [PubMed: 22101433]

Appendix

Contributions

The Cancer Genome Atlas research network contributed collectively to this study. Biospecimens were provided by the tissue source sites and processed by the Biospecimen Core Resource. Data generation and analyses were performed by the genome-sequencing centers, cancer genome-characterization centers and genome data analysis centers. All data were released through the Data Coordinating Center. Project activities were coordinated by the NCI and NHGRI project teams. We also acknowledge the following TCGA investigators of the Kidney Analysis Working Group who contributed substantially to the analysis and writing of this manuscript: **Project leaders:** Richard A. Gibbs, W. Marston Linehan. **Data Coordinator:** Margaret Morgan. **Analysis Coordinators:** Chad J. Creighton, Roel G. W. Verhaak. **Manuscript Coordinators:** Richard A. Gibbs, Chad J. Creighton. **Writing Team:** W. Marston Linehan, Chad J. Creighton, W. Kimryn Rathmell, Roel G. W. Verhaak, Richard A. Gibbs. **DNA Sequence analysis:** David A Wheeler, Kristian Cibulskis. **mRNA analysis:** Roel G. W. Verhaak, A. Rose Brannon, W. Kimryn Rathmell, Wandaliz Torres-Garcia. **microRNA analysis:** A. Gordon Robertson, Andy Chu, Preethi H. Gunaratne. **DNA methylation analysis:** Hui Shen, Peter W. Laird. **Copy number analysis:** Rameen Beroukhi, Sabina Signoretti. **Protein analysis:** Dimitra Tsavachidou, Yiling Lu, Gordon B Mills. **Pathway/Integrated Analysis:** Rehan Akbani, Giovanni Ciriello, Chad J. Creighton, Suzanne S. Fei, Anders Jacobsen, Evan O. Paull, Ben Raphael, Shelia Reynolds, Christopher J. Ricketts, Nikolaus Schultz, Joshua M. Stuart, Fabio Vandin. **Clinical Data:** W. Kimryn Rathmell, A. Ari Hakimi, Johanna Gardener, Candace Shelton. **Pathology and Clinical Expertise:** James Hsieh, Marston W. Linehan, Pheroze Tamboli, W. Kimryn Rathmell, Victor Reuter.

Analysis Working Group

Baylor College of Medicine – Chad J. Creighton^(1, 2), Margaret Morgan⁽¹⁾, Preethi Gunaratne^(1, 3), David Wheeler⁽¹⁾, Richard Gibbs⁽¹⁾, *BC Cancer Agency* – A. Gordon Robertson⁽⁴⁾, Andy Chu⁽⁴⁾, *Broad Institute* - Rameen Beroukhim^(5, 6), Kristian Cibulskis⁽⁶⁾, *Brigham and Women's Hospital* - Sabina Signoretti⁽⁷⁾, *Brown University* - Fabio Vandin⁽⁸⁾, Hsin-Ta Wu⁽⁸⁾, Benjamin J. Raphael⁽⁸⁾, *The University of Texas M.D. Anderson Cancer Center* - Roel G.W. Verhaak⁽⁹⁾, Pheroze Tamboli⁽¹⁰⁾, Wandaliz Torres-Garcia⁽⁹⁾, Rehan Akbani⁽⁹⁾, John N. Weinstein⁽⁹⁾, *Memorial Sloan-Kettering Cancer Center* - Victor Reuter⁽¹¹⁾, James J Hsieh⁽¹²⁾, A. Rose Brannon⁽¹¹⁾, A. Ari Hakimi⁽¹²⁾, Anders Jacobsen⁽¹³⁾, Giovanni Ciriello⁽¹³⁾, Boris Reva⁽¹³⁾, *National Cancer Institute* – Christopher J. Ricketts⁽¹⁴⁾, W. Marston Linehan⁽¹⁴⁾, *UC Santa Cruz* - Joshua M. Stuart⁽¹⁵⁾, *University of North Carolina, Chapel Hill* - W. Kimryn Rathmell⁽¹⁶⁾, *University of Southern California* - Hui Shen⁽¹⁷⁾, Peter W. Laird⁽¹⁷⁾.

Genome Sequencing Centers

Baylor College of Medicine - Donna Muzny⁽¹⁾, Caleb Davis⁽¹⁾, Margaret Morgan⁽¹⁾, Liu Xi⁽¹⁾, Kyle Chang⁽¹⁾, Nipun Kakkar⁽¹⁾, Lisa R. Treviño⁽¹⁾, Susan Benton⁽¹⁾, Jeffrey G. Reid⁽¹⁾, Donna Morton⁽¹⁾, Harsha Doddapaneni⁽¹⁾, Yi Han⁽¹⁾, Lora Lewis⁽¹⁾, Huyen Dinh⁽¹⁾, Christie Kovar⁽¹⁾, Yiming Zhu⁽¹⁾, Jireh Santibanez⁽¹⁾, Min Wang⁽¹⁾, Walker Hale⁽¹⁾, Divya Kalra⁽¹⁾, Chad J. Creighton^(1, 2), David A. Wheeler⁽¹⁾, Richard Gibbs⁽¹⁾, *Broad Institute* - Andrew Cherniack⁽⁶⁾, Barbara Tabak⁽⁶⁾, Gad Getz⁽⁶⁾, Gordon Saksena⁽⁶⁾, Jeff Gentry⁽⁶⁾, Kristin Ardlie⁽⁶⁾, Robert C. Onofrio⁽⁶⁾, Scott L. Carter⁽⁶⁾, Stacey B. Gabriel⁽⁶⁾, Kristian Cibulskis⁽⁶⁾, Carrie Sougnez⁽⁶⁾, Steve Schumacher⁽⁶⁾, Matthew Meyerson⁽⁶⁾.

Genome Characterization Centers

Broad Institute - Rameen Beroukhim^(5, 6), *BC Cancer Agency* - A. Gordon Robertson⁽⁴⁾, Andy Chu⁽⁴⁾, Hye-Jung E. Chun⁽⁴⁾, Andrew J. Mungall⁽⁴⁾, Payal Sipahimalani⁽⁴⁾, Dominik Stoll⁽⁴⁾, Adrian Ally⁽⁴⁾, Miruna Balasundaram⁽⁴⁾, Yaron S.N. Butterfield⁽⁴⁾, Rebecca

¹Human Genome Sequencing Center, Baylor College of Medicine, Houston, TX 77030.

²Dan L Duncan Cancer Center, Baylor College of Medicine, Houston, TX 77030.

³Department of Biology & Biochemistry, University of Houston, Houston, TX 77204 USA

⁴Canada's Michael Smith Genome Sciences Centre, BC Cancer Agency, Vancouver, BC V5Z, Canada.

⁵Department of Medicine, Harvard Medical School, Boston, MA 02215 USA.

⁶The Eli and Edythe L. Broad Institute of Massachusetts Institute Of Technology and Harvard University, Cambridge, MA 02142 USA.

⁷Department of Pathology, Harvard Medical School, Boston, MA 02215 USA.

⁸Department of Computer Science, Brown University, Providence, RI 02912 USA.

⁹Department of Bioinformatics and Computational Biology, The University of Texas MD Anderson Cancer Center, Houston, TX 77030 USA.

¹⁰Department of Pathology, The University of Texas MD Anderson Cancer Center, Houston, TX 77030 USA.

¹¹Department of Pathology, Memorial Sloan-Kettering Cancer Center, New York, NY 10065 USA.

¹²Human Oncology and Pathogenesis Program, Memorial Sloan-Kettering Cancer Center, New York, NY 10065 USA.

¹³Computational Biology Center, Memorial Sloan-Kettering Cancer Center, New York, NY 10065 USA.

¹⁴Urologic Oncology Branch, Center for Cancer Research, National Cancer Institute, Bethesda, MD 20892 USA.

¹⁵Department of Biomolecular Engineering and Center for Biomolecular Science and Engineering, University of California Santa Cruz, Santa Cruz, CA 95064 USA.

¹⁶Lineberger Comprehensive Cancer Center, University of North Carolina at Chapel Hill, Chapel Hill, NC 27599 USA.

¹⁷USC Epigenome Center, University of Southern California, Los Angeles, CA 90033 USA.

Carlsen⁽⁴⁾, Candace Carter⁽⁴⁾, Eric Chuah⁽⁴⁾, Robin J.N. Coope⁽⁴⁾, Noreen Dhalla⁽⁴⁾, Sharon Gorski⁽⁴⁾, Ranabir Guin⁽⁴⁾, Carrie Hirst⁽⁴⁾, Martin Hirst⁽⁴⁾, Robert A. Holt⁽⁴⁾, Chandra Lebovitz⁽⁴⁾, Darlene Lee⁽⁴⁾, Haiyan I. Li⁽⁴⁾, Michael Mayo⁽⁴⁾, Richard A. Moore⁽⁴⁾, Erin Pleasance⁽⁴⁾, Patrick Plettner⁽⁴⁾, Jacqueline E. Schein⁽⁴⁾, Arash Shafiei⁽⁴⁾, Jared R. Slobodan⁽⁴⁾, Angela Tam⁽⁴⁾, Nina Thiessen⁽⁴⁾, Richard J. Varhol⁽⁴⁾, Natasja Wye⁽⁴⁾, Yongjun Zhao⁽⁴⁾, Inanc Birol⁽⁴⁾, Steven J.M. Jones⁽⁴⁾, Marco A. Marra⁽⁴⁾, *University of North Carolina, Chapel Hill* - J. Todd Auman⁽¹⁸⁾, Donghui Tan⁽¹⁹⁾, Corbin D. Jones⁽²⁰⁾, Katherine A. Hoadley^(16, 21, 22), Piotr A. Mieczkowski⁽²²⁾, Lisle E. Mose⁽²¹⁾, Stuart R. Jefferys⁽²²⁾, Michael D. Topal^(21, 22), Christina Liquori⁽¹⁶⁾, Yidi J. Turman⁽¹⁶⁾, Yan Shi⁽¹⁶⁾, Scot Waring⁽¹⁶⁾, Elizabeth Buda⁽¹⁶⁾, Jesse Walsh⁽¹⁶⁾, Junyuan Wu⁽¹⁶⁾, Tom Bodenheimer⁽¹⁶⁾, Alan P. Hoyle⁽¹⁶⁾, Janae V. Simons⁽¹⁶⁾, Mathew G. Soloway⁽¹⁶⁾, Saianand Balu⁽¹⁶⁾, Joel S. Parker⁽¹⁶⁾, D. Neil Hayes^(16, 23), Charles M. Perou^(16, 21, 22), *Harvard Medical School* - Raju Kucherlapati^(24, 25), Peter Park⁽²⁵⁻²⁷⁾, *University of Southern California and Johns Hopkins University* - Hui Shen⁽¹⁷⁾, Timothy Triche Jr.⁽¹⁷⁾, Daniel J. Weisenberger⁽¹⁷⁾, Phillip H. Lai⁽¹⁷⁾, Moiz S. Bootwalla⁽¹⁷⁾, Dennis T. Maglinte⁽¹⁷⁾, Swapna Mahurkar⁽¹⁷⁾, Benjamin P. Berman⁽¹⁷⁾, David J. Van Den Berg⁽¹⁷⁾, Leslie Cope⁽²⁸⁾, Stephen B. Baylin⁽²⁸⁾, Peter W. Laird⁽¹⁷⁾.

Genome Data Analysis

Baylor College of Medicine – Chad J. Creighton^(1, 2), *Brown University* - Fabio Vandin⁽⁸⁾, Hsin-Ta Wu⁽⁸⁾, Benjamin J. Raphael⁽⁸⁾, *Institute for Systems Biology* - Sheila M. Reynolds⁽²⁹⁾, *The University of Texas M.D. Anderson Cancer Center* - Roel G.W. Verhaak⁽⁹⁾, Wandaliz Torres-Garca⁽⁹⁾, Rahul Vegesna⁽⁹⁾, Hoon Kim⁽⁹⁾, Wei Zhang⁽⁹⁾, David Cogdell⁽⁹⁾, Eric Jonasch⁽⁹⁾, Zhiyong Ding⁽⁹⁾, Yiling Lu⁽³⁰⁾, Rehan Akbani⁽⁹⁾, Nianxiang Zhang⁽⁹⁾, Anna K. Unruh⁽⁹⁾, Tod D. Casasent⁽⁹⁾, Chris Wakefield⁽⁹⁾, Dimitra Tsavachidou⁽³⁰⁾, Lynda Chin⁽³¹⁾, Gordon B. Mills⁽³⁰⁾, John N. Weinstein⁽⁹⁾, *Memorial Sloan-Kettering Cancer Center* - Anders Jacobsen⁽¹³⁾, A. Rose Brannon⁽¹¹⁾, Giovanni Ciriello⁽¹³⁾, Nikolaus Schultz⁽¹³⁾, A Ari Hakimi⁽¹²⁾, Boris Reva⁽¹³⁾, Yevgeniy Antipin⁽¹³⁾, Jianjiong Gao⁽¹³⁾, Ethan Cerami⁽¹³⁾, Benjamin Gross⁽¹³⁾, B. Arman Aksoy⁽¹³⁾, Rileen Sinha⁽¹³⁾, Nils Weinhold⁽¹³⁾, S. Onur Sumer⁽¹³⁾, Barry S. Taylor⁽¹³⁾, Ronglai Shen⁽¹³⁾, Irina Ostrovnya⁽³²⁾, James J Hsieh⁽¹²⁾, Michael F. Berger⁽¹¹⁾, Marc Ladanyi⁽¹²⁾, Chris Sander⁽¹³⁾, *Oregon Health & Science University* - Suzanne S. Fei⁽³³⁾,

¹⁸Eshelman School of Pharmacy, University of North Carolina at Chapel Hill, Chapel Hill, NC 27599 USA.

¹⁹Carolina Center for Genome Sciences, University of North Carolina at Chapel Hill, Chapel Hill, NC 27599 USA.

²⁰Department of Biology, University of North Carolina at Chapel Hill, Chapel Hill, NC 27599 USA.

²¹Department of Pathology and Laboratory Medicine, University of North Carolina at Chapel Hill, Chapel Hill, NC 27599 USA.

²²Department of Genetics, University of North Carolina at Chapel Hill, Chapel Hill, NC 27599 USA.

²³Department of Internal Medicine, Division of Medical Oncology, University of North Carolina at Chapel Hill, Chapel Hill, NC 27599 USA.

²⁴Department of Genetics, Harvard Medical School, Boston, MA 02215 USA.

²⁵Division of Genetics, Brigham and Women's Hospital, Boston, MA 02115 USA.

²⁷Informatics Program, Children's Hospital, Boston, MA 02115 USA.

²⁸Cancer Biology Division, The Sidney Kimmel Comprehensive Cancer Center at Johns Hopkins University, Baltimore, MD 21231 USA.

²⁹Institute for Systems Biology, Seattle, WA 98109 USA.

³⁰Department of Systems Biology, The University of Texas MD Anderson Cancer Center, Houston, TX 77030 USA.

³¹Department of Genomic Medicine, University of Texas MD Anderson Cancer Center, Houston, TX 77054.

³²Department of Epidemiology and Biostatistics, Memorial Sloan-Kettering Cancer Center, New York, NY 10065 USA.

Andrew Stout⁽³³⁾, Paul T Spellman⁽³³⁾, *Stanford University* - Daniel L. Rubin⁽³⁴⁾, Tiffany T. Liu⁽³⁴⁾, *UC Santa Cruz* - Joshua M. Stuart⁽¹⁵⁾, Sam Ng⁽¹⁵⁾, Evan O. Paull⁽¹⁵⁾, Daniel Carlin⁽¹⁵⁾, Theodore Goldstein⁽¹⁵⁾, Peter Waltman⁽¹⁵⁾, Kyle Ellrott⁽¹⁵⁾, Jing Zhu⁽¹⁵⁾, David Haussler^(15, 35), *University of Houston* – Preethi H Gunaratne^(1, 3), Weimin Xiao⁽³⁾.

Biospecimen Core Resource

International Genomics Consortium - Candace Shelton⁽³⁶⁾, Johanna Gardner⁽³⁶⁾, Robert Penny⁽³⁶⁾, Mark Sherman⁽³⁶⁾, David Mallery⁽³⁶⁾, Scott Morris⁽³⁶⁾, Joseph Paulauskis⁽³⁶⁾, Ken Burnett⁽³⁶⁾, Troy Shelton⁽³⁶⁾.

Tissue Source Sites

Brigham and Women's Hospital - Sabina Signoretti⁽⁷⁾, *Dana-Farber Cancer Institute* - William G. Kaelin⁽⁵⁾, Toni Choueiri⁽⁵⁾, *Georgetown University*- Michael B. Atkins⁽³⁷⁾, *International Genomics Consortium* - Robert Penny⁽³⁸⁾, Ken Burnett⁽³⁸⁾, David Mallery⁽³⁸⁾, Erin Curley⁽³⁸⁾, *Memorial Sloan-Kettering Cancer Center* - Satish Tickoo⁽¹¹⁾, Victor Reuter⁽¹¹⁾, *University of North Carolina at Chapel Hill* - W. Kimryn Rathmell⁽¹⁶⁾, Leigh Thorne⁽¹⁶⁾, Lori Boice⁽¹⁶⁾, Mei Huang⁽¹⁶⁾, Jennifer C. Fisher⁽¹⁶⁾. *National Cancer Institute* - W. Marston Linehan⁽¹⁴⁾, Cathy D. Vocke⁽¹⁴⁾, James Peterson⁽¹⁴⁾, Robert Worrell⁽¹⁴⁾, Maria J. Merino⁽¹⁴⁾, Laura S. Schmidt^(14, 39), *The University of Texas M.D. Anderson Cancer Center* - Pheroze Tamboli⁽¹⁰⁾, Bogdan A. Czerniak⁽¹⁰⁾, Kenneth D. Aldape⁽¹⁰⁾, Christopher G. Wood⁽⁴⁰⁾. *Fox Chase Cancer Center* - Jeff Boyd⁽⁴¹⁾, JoEllen Weaver⁽⁴¹⁾, *Helen F Graham Cancer Center at Christiana Care* - Mary V. Iacocca⁽⁴²⁾, Nicholas Petrelli⁽⁴²⁾, Gary Witkin⁽⁴²⁾, Jennifer Brown⁽⁴²⁾, Christine Czerwinski⁽⁴²⁾, Lori Huelsenbeck-Dill⁽⁴²⁾, Brenda Rabeno⁽⁴²⁾, *Penrose-St. Francis Health Services* – Jerome Myers⁽⁴³⁾, Carl Morrison⁽⁴³⁾, Julie Bergsten⁽⁴³⁾, John Eckman⁽⁴³⁾, Jodi Harr⁽⁴³⁾, Christine Smith⁽⁴³⁾, Kelinda Tucker⁽⁴³⁾, Leigh Anne Zach⁽⁴³⁾, *Roswell Park Cancer Institute* - Wiam Bshara⁽⁴⁴⁾, Carmelo Gaudio⁽⁴⁴⁾, Carl Morrison⁽⁴⁴⁾, *University of Pittsburgh* - Rajiv Dhir⁽⁴⁵⁾, Jodi Maranchie⁽⁴⁵⁾, Joel Nelson⁽⁴⁵⁾, Anil Parwani⁽⁴⁵⁾, *Cureline* – Olga Potapova⁽⁴⁶⁾, *St. Petersburg City Clinical Oncology Dispensary* - Konstantin Fedosenko⁽⁴⁷⁾.

³³Department of Molecular & Medical Genetics, Oregon Health & Science University, Portland, OR 97239 USA.

³⁴Department of Radiology, Stanford University Medical Center, Stanford, CA 94305, USA.

³⁵Howard Hughes Medical Institute, University of California Santa Cruz, Santa Cruz, CA 95064 USA.

³⁶The Research Institute at Nationwide Children's Hospital, Columbus, OH 43205.

³⁷Georgetown-Lombardi Comprehensive Cancer Center, Georgetown University, Washington D.C. 20057 USA.

³⁸International Genomics Consortium, Phoenix, AZ 85004 USA.

³⁹Basic Science Program, SAIC-Frederick, Inc., Frederick National Lab, Frederick, MD 21702 USA.

⁴⁰Department of Urology, The University of Texas MD Anderson Cancer Center, Houston, TX 77030 USA.

⁴¹Cancer Biology Program, Fox Chase Cancer Center, Philadelphia, PA USA 19111.

⁴²Helen F. Graham Cancer Center, Christiana Care, Newark, Delaware 19713 USA.

⁴³Penrose-St. Francis Health Services, Colorado Springs, CO USA 80907.

⁴⁴Department of Pathology, Roswell Park Cancer Institute, Buffalo, NY 14263 USA.

⁴⁵Department of Pathology, University of Pittsburgh, Pittsburgh, PA, 15213 USA.

⁴⁶Cureline, Inc. South San Francisco, CA 94080 USA.

⁴⁷St. Petersburg City Clinical Oncology Dispensary, St. Petersburg 198255, Russia.

Disease working group

Brigham and Women's Hospital - Sabina Signoretti⁽⁷⁾, *Dana-Farber Cancer Institute* - William G. Kaelin⁽⁵⁾, *Georgetown University* - Michael B. Atkins⁽³⁷⁾, *Memorial Sloan-Kettering Cancer Center* - Satish Tickoo⁽¹¹⁾, Victor Reuter⁽¹¹⁾, *National Cancer Institute* - W. Marston Linehan⁽¹⁴⁾, Cathy D. Vocke⁽¹⁴⁾, James Peterson⁽¹⁴⁾, Maria J. Merino⁽¹⁴⁾, Laura S. Schmidt^(14, 39), *The University of Texas M.D. Anderson Cancer Center* - Pheroze Tamboli⁽¹⁰⁾, *Weill Cornell Medical College* - Juan M. Mosquera⁽⁴⁸⁾, Mark A. Rubin⁽⁴⁸⁾, *Massachusetts General Hospital* - Michael L. Blute⁽⁴⁹⁾, *University of North Carolina, Chapel Hill* - W. Kimryn Rathmell⁽¹⁶⁾

Data Coordination Center

Todd Pihl⁽⁵⁰⁾, Mark Jensen⁽⁵⁰⁾, Robert Sfeir⁽⁵⁰⁾, Ari Kahn⁽⁵⁰⁾, Anna Chu⁽⁵⁰⁾, Prachi Kothiyal⁽⁵⁰⁾, Zhining Wang⁽⁵⁰⁾, Eric Snyder⁽⁵⁰⁾, Joan Pontius⁽⁵⁰⁾, Brenda Ayala⁽⁵⁰⁾, Mark Backus⁽⁵⁰⁾, Jessica Walton⁽⁵⁰⁾, Julien Baboud⁽⁵⁰⁾, Dominique Berton⁽⁵⁰⁾, Matthew Nicholls⁽⁵⁰⁾, Deepak Srinivasan⁽⁵⁰⁾, Rohini Raman⁽⁵⁰⁾, Stanley Girshik⁽⁵⁰⁾, Peter Kigonya⁽⁵⁰⁾, Shelley Alonso⁽⁵⁰⁾, Rashmi Sanbhadti⁽⁵⁰⁾, Sean Barletta⁽⁵⁰⁾, David Pot⁽⁵⁰⁾

Project Team

National Cancer Institute - Margi Sheth⁽⁵¹⁾, Kenna R. Mills Shaw⁽⁵¹⁾, John A. Demchok⁽⁵¹⁾, Tanja Davidsen⁽⁵¹⁾, Liming Yang⁽⁵¹⁾, Roy W. Tarnuzzer⁽⁵¹⁾, Jiashan Zhang⁽⁵¹⁾, Greg Eley⁽⁵²⁾, Martin L. Ferguson⁽⁵³⁾, *National Human Genome Research Institute* - Mark S. Guyer⁽⁵⁴⁾, Bradley A. Ozenberger⁽⁵⁴⁾, Heidi J. Sofia⁽⁵⁴⁾.

⁴⁸Department of Pathology and Laboratory Medicine, Weill Cornell College of Medicine, New York, NY 10065 USA.

⁴⁹Department of Urology, Massachusetts General Hospital, Boston, MA 02114 USA.

⁵⁰SRA International, 4300 Fair Lakes Court, Fairfax, VA 22033.

⁵¹The Cancer Genome Atlas Program Office, Center for Cancer Genomics, National Cancer Institute, Bethesda, MD.

⁵²TCGA Consultant, Scimentis, LLC, Atlanta, GA.

⁵³MLF Consulting, Arlington, MA 02474 USA.

⁵⁴National Human Genome Research Institute, National Institutes of Health, Bethesda, MD, 20892.

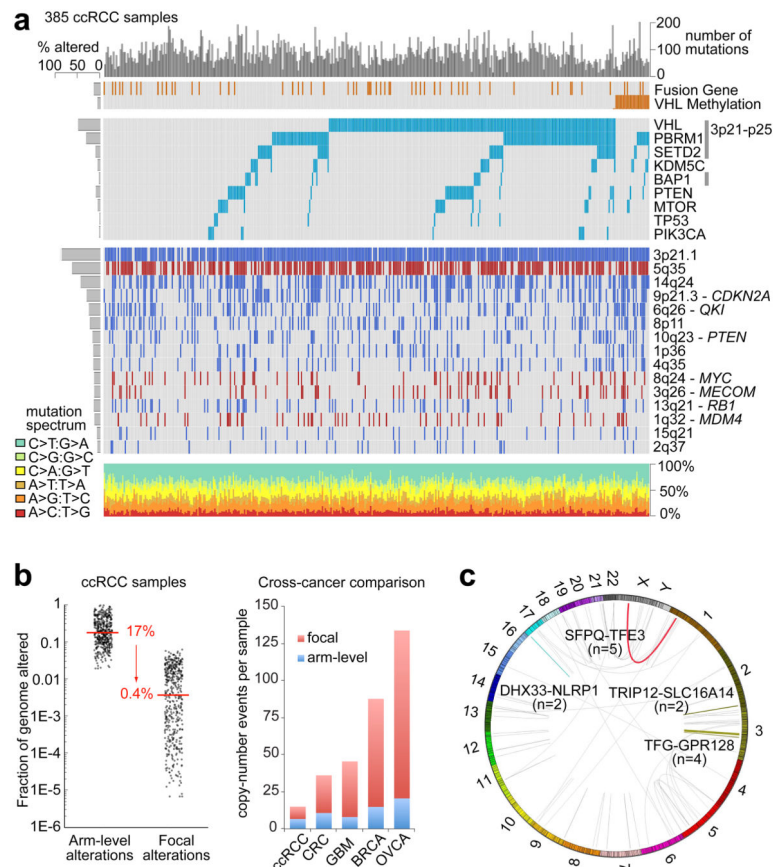


Figure One. Somatic alterations in ccRCC

(a) Top histogram, mutation events per sample; left histogram, samples affected per alteration. Upper heat map, distribution of fusion transcripts and *VHL* methylation across samples (n=385 samples, with overlapping exome/CNA/RNA-seq/Methylation data); middle heatmap, mutation events; bottom heatmap, copy number gains (red) and losses (blue). Lower chart, mutation spectrum by indicated categories. (b) Left panel, frequency of arm level copy number alterations versus focal copy number alterations. Right panel, comparison of the average numbers of arm level and focal copy number changes in ccRCC, colon cancer (CRC), glioblastoma (GBM), breast cancer (BRCA) and ovarian cancer (OVCA). (c) Circos plot of fusion transcripts identified in 416 samples of ccRCC, with recurrent fusions highlighted.

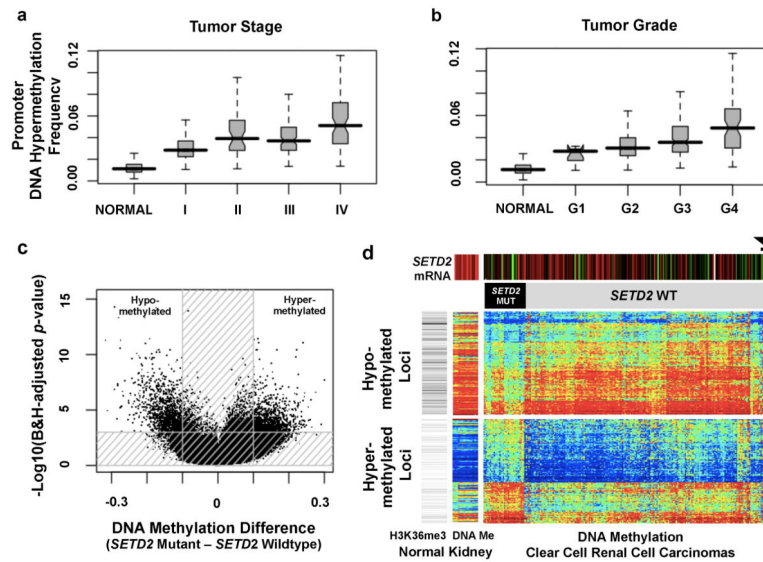


Figure Two. DNA methylation and ccRCC

(a–b) Overall promoter DNA hypermethylation frequency in the tumor increases with rising stage (a) and grade (b). The promoter DNA hypermethylation frequency is calculated as the percentage of CpG loci hypermethylated among 15,101 loci which are unmethylated in the normal kidney tissue and normal white blood cells (boxplots, median with 95% confidence interval). (c) Volcano plots showing a comparison of DNA methylation for *SETD2* mutant versus non-mutant tumors (n=224, Human Methylation 450 platform). Unshaded area: CpG loci with Benjamini-Hochberg FDR=0.001 and difference in mean beta value >0.1 (n=2,557). (d) Heatmap showing CpG loci with *SETD2* mutation-associated DNA methylation (from part c); blue to red indicates low to high DNA methylation. The loci are split into those hypomethylated (top panel; n=1,251) or hypermethylated (bottom panel; n=1,306) in *SETD2* mutants. Top color bars indicate *SETD2* mRNA expression (red: high, green: low) and *SETD2* mutation status. Gray-scale row-side color bar on left-hand side represents the relative number of overlapping reads, based on H3K36me3 ChIP-seq experiment in normal adult kidney (<http://nihroadmap.nih.gov/epigenomics/>); black, high read count. DNA methylation patterns include 14 normal kidney samples. Among the tumors without *SETD2* mutations, six (arrowhead) have both the signature pattern of *SETD2* mutation and low *SETD2* mRNA expression.

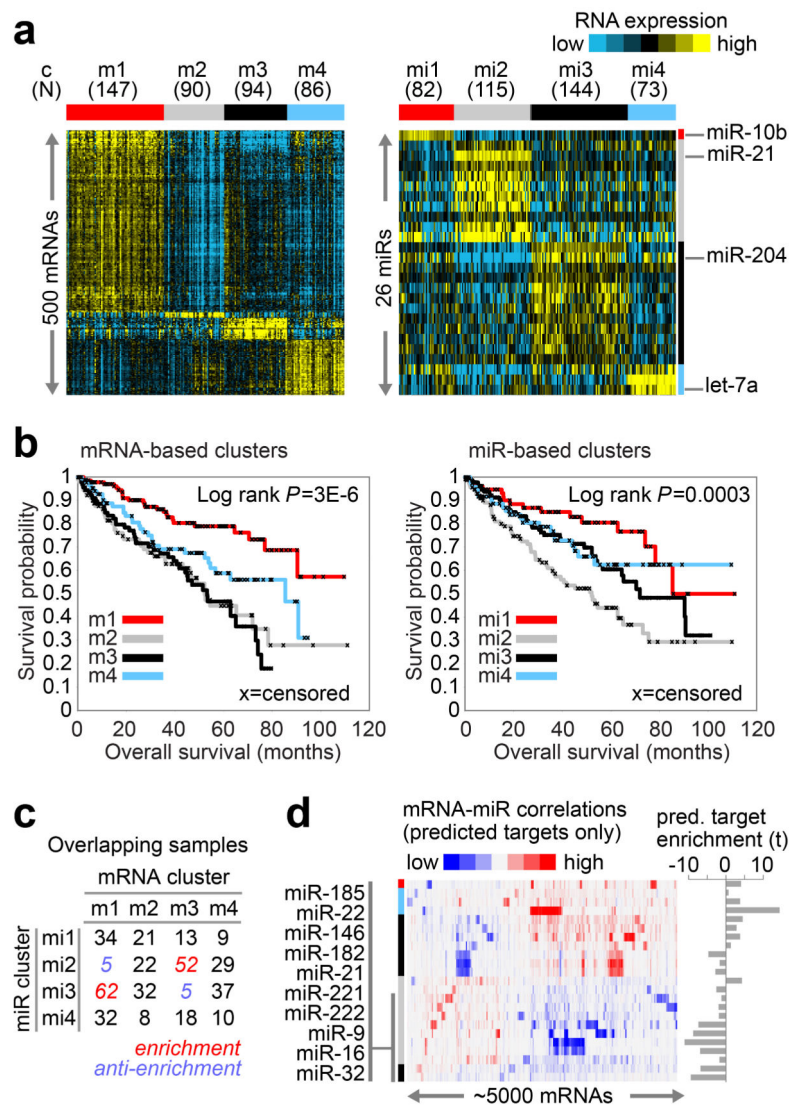


Figure Three. mRNA and miRNA patterns reflect molecular subtypes of ccRCC
(a) By unsupervised analyses, tumors separated into four sample groups (i.e. “clusters”), based on either differentially expressed mRNA patterns (left panel, showing 500 representative genes: m1–4) or differentially expressed miRNA patterns (right panel, showing 26 representative miRNAs: mi1–4). **(b)** Significant differences in patient survival were identified among either the mRNA-based clusters (left panel) or the miRNA-based clusters (right panel). **(c)** Numbers of samples overlapping between the two sets of clusters, with significant concordance observed between m1 and mi3 and between m3 and mi2; Red, significant overlap ($P < 1E-5$, chi-squared test). **(d)** mRNA-miRNA correlations, for predicted targeting interactions. Rows indicate miRNAs from part a (indicated by cluster specific color bar); columns, mRNAs (5000 differentially regulated genes selected for average RPKM > 10 and at least one predicted miRNA interaction); mRNA-miRNA entries with no predicted targeting show as white. To the right of the correlation matrix, t-statistics (Spearman’s rank) indicate group target enrichment.

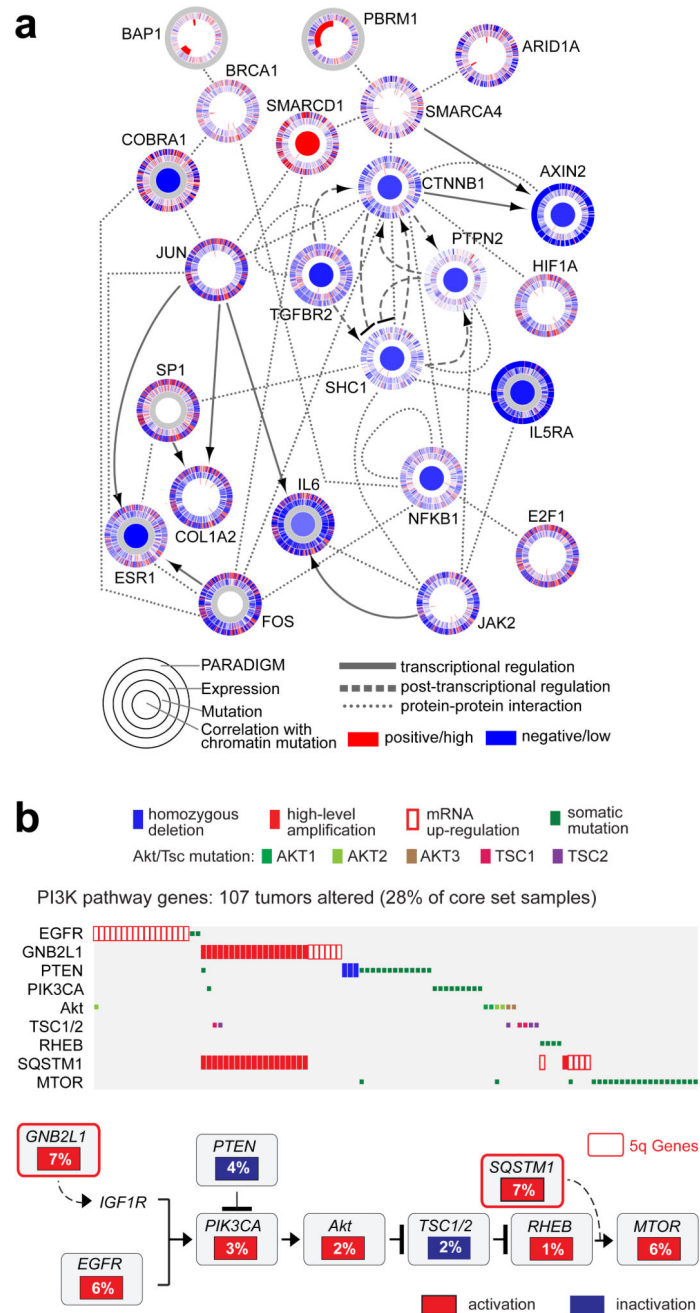


Figure Four. Genomically-altered pathways in ccRCC

(a) Alterations in chromatin remodeling genes were predicted to impact a large network of genes and pathways (larger implicated network in supplemental). Each gene is depicted as a multi-ring circle with various levels of data, plotted such that each ‘spoke’ in the ring represents a single patient sample (same sample ordering for all genes). ‘PARADIGM’ ring, bioinformatically inferred levels of gene activity (red, higher activity); ‘Expression’, mRNA levels relative to normal (red, high); ‘Mutation’, somatic event; center, correlation of gene expression or activity to mutation events in chromatin-related genes (red, positive). Protein-protein relationships inferred using public resources. (b) For the PI3K/Akt/mTOR pathway

(altered in ~28% of tumors), the MEMo algorithm identified a pattern of mutually exclusive gene alterations (somatic mutations, copy alterations, and aberrant mRNA expression) targeting multiple components, including 2 genes from the recurrent amplicon on 5q35.3. The alteration frequency and inferred alteration type (blue for inactivation, and red for activation) is shown for each gene in the pathway diagram.

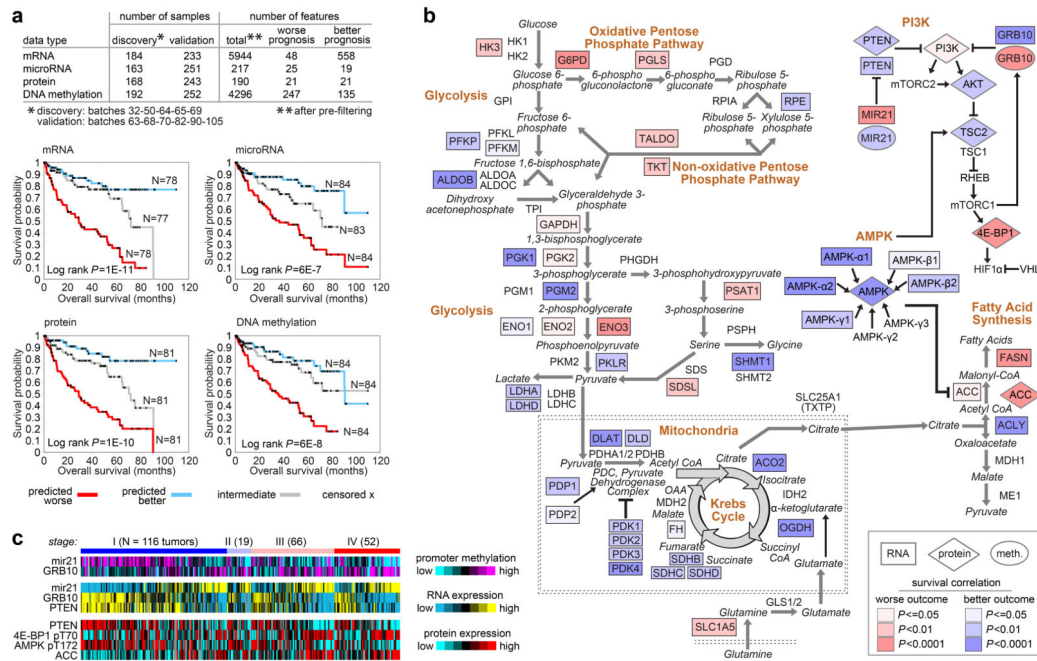


Figure Five. Molecular correlates of patient survival involve metabolic pathways

(a) Sample profiles were separated into discovery and validation subsets, with the top survival correlates within the discovery subset being defined for each of the four platforms examined (mRNA, microRNA, protein, DNA methylation). Kaplan-Meier plots show results of applying the four prognostic signatures to the validation subset, comparing survival for patients with predicted higher risk (red, top third of signature scores), lower risk (blue, bottom third), or intermediate risk (gray, middle third); successful predictions were observed in each case. (b) When viewed in the context of metabolism, the molecular survival correlates highlight a widespread metabolic shift, with tumors altering their usage of key pathways and metabolites (red and blue shading representing the correlation of increased gene expression with worse or better survival respectively, univariate Cox based on extended cohort). Worse survival correlates with up-regulation of pentose phosphate pathway genes (*G6PH*, *PGLS*, *TALDO* and *TKT*), fatty acid synthesis genes (*ACC* and *FASN*), and PI3K pathway enhancing genes (*miR-21*). Better survival correlates with up-regulation of AMPK complex genes, multiple Krebs cycle genes, and PI3K pathway inhibitors (*PTEN*, *TSC2*). Additionally, specific promoter methylation events, including hypermethylation of PI3K pathway repressor *GRB10*, associate with outcome. (c) Heat map of selected key features from the metabolic shift schematic (b) demonstrating coordinate expression by stage at DNA methylation, RNA, and protein levels (data from validation subset).